Electric Power Systems Research 144 (2017) 233–242

Contents lists available at ScienceDirect

Electric Power Systems Research

journal homepage: www.elsevier.com/locate/epsr

Modeling power networks using dynamic phasors in the *dq*0 reference frame

Yoash Levron[a,*], Juri Belikov[b]

[a] The Andrew and Erna Viterbi Faculty of Electrical Engineering, Technion—Israel Institute of Technology, Haifa 3200003, Israel
[b] Faculty of Mechanical Engineering, Technion—Israel Institute of Technology, Haifa 3200003, Israel

ARTICLE INFO

Article history:
Received 26 July 2016
Received in revised form
20 November 2016
Accepted 28 November 2016

Keywords:
Quasi static
Average signals
Dynamic phasors
Inter-area oscillations
Multi-machine
Stability

ABSTRACT

The dynamic behavior of large power systems has been traditionally studied by means of time-varying phasors, under the assumption that the system is quasi-static. However, with increasing integration of fast renewable and distributed sources into power grids, this assumption is becoming increasingly inaccurate. In this paper, we present a dynamic model of general transmission and distribution networks that uses dynamic phasors in the *dq*0 reference frame. The model is formulated in the frequency domain, and is based on the network frequency dependent admittance matrix. We also present a simplified version of this model that is obtained by a first-order Taylor approximation of the dynamic equations. The proposed models extend the quasi-static model to higher frequencies, while employing *dq*0 signals that are static at steady-state, and therefore combine the advantages of high bandwidth and a well-defined operating point. The models are verified numerically using the 9-, 30-, and 118-bus test-case networks. Simulations show that frequency responses of all models coincide at low frequencies and diverge at high frequencies. In addition, responses of the *dq*0 model in the time domain and in the *abc* reference frame are very close to those of the transient model.

1. Introduction

Dynamic processes occurring in large electric power systems are modeled at varying levels of abstraction [1,2]. In simple static models, voltages and currents are assumed to be sinusoidal, and are represented by phasors. The network is typically described in this case by the power flow equations. On the other extreme, transient models describe the system using nonlinear differential equations, which are solved numerically in the time domain [3–8]. A third type of model, based on time-varying phasors, is called the average-value, dynamic or quasi-static model [2]. This model is sufficiently accurate as long as phasors are slowly changing in comparison to the system frequency [9,10]. A key advantage of the quasi-static model is that it enables long numeric step times, and hence can accelerate the simulation process. In addition, since the quasi-static model employs phasors instead of sinusoidal AC signals, the system operating point is well-defined, a property which considerably simplifies stability studies. Due to these properties, quasi-static models have been used extensively in the analysis of dynamic interactions that occur in time frames of seconds to minutes, and have historically enabled studies of machines stability, inter-area oscillation, and slow dynamic phenomena [1–3,11].

In recent years, with the emergence of small distributed generators and fast power electronics based devices, the assumption of quasi-static phasors is becoming increasingly inaccurate. Due to these emerging technologies, voltage and current signals can contain high harmonic components, and can exhibit fast amplitude and phase variations [9]. These developments have led to a new class of models based on dynamic phasors. The concept of dynamic phasors has emerged from averaging techniques employed in power electronics, and has been extended to three-phase systems [12]. Dynamic phasors generalize the idea of quasi-static phasors, and represent voltage and current signals by Fourier series expansions in which the harmonic components are evaluated over a moving time window [13]. This approach offers the benefits of a phasor based analysis, high accuracy, and fast simulations [14,15].

Due to these properties, dynamic phasors have been used in the analysis of synchronous and induction machines [12,16], HVDC systems [14,17,18], FACTS devices [10], sub-synchronous resonance [19,20], asymmetric systems [12,21], and asymmetric faults [16,22]. For

* Corresponding author.
E-mail addresses: yoashl@ee.technion.ac.il (Y. Levron), juri.belikov@ttu.ee (J. Belikov).

http://dx.doi.org/10.1016/j.epsr.2016.11.024
0378-7796/

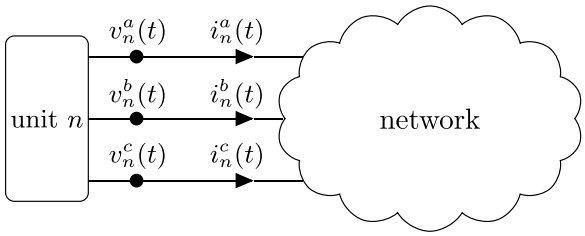

Fig. 1. A unit in the network, showing signals in the *abc* reference frame.

instance, a dynamic phasor model of a line commutated HVDC converter is presented in [14]. The model represents the low-frequency dynamics of the converter, and has lower computational requirements than a conventional transient model. A dynamic phasor representation of an unbalanced radial distribution system is presented in [21], where various components including a photovoltaic source and an induction machine are modeled, and dynamic interaction of these components is shown. A simulator based on dynamic phasors has been developed in [15,23], which uses differential switched-algebraic state-reset equations to describe the system components. The simulation tool combines advantages of transient stability and electro-magnetic simulation programs, and is demonstrated on the IEEE 39 bus test-case network. Work [24] extends the dynamic phasor concept to multi-generator, multi-frequency systems. The theory presented in [24] enables study of electric power systems without assuming a single frequency. The proposed approach is validated on a twin-generator system, and can be extended to larger networks. In addition, dynamic phasors are utilized in state estimation [25–29], in systems with varying frequencies [30], and also in microgrids [31].

These recent works are mainly focused on modeling specific generators and loads, and do not provide a complete model of large transmission networks. To bridge this gap, this paper presents a dynamic model of general transmission and distribution networks using dynamic phasors in the *dq*0 reference frame, and shows how this model can be implemented in practice using time-domain state equations. The first model presented in this work is formulated in the frequency domain, and is based on the network frequency dependent admittance matrix. Since a direct numeric implementation of this model is challenging in general, we present a simplified version of it called the *first-order dq*0 model, which is obtained by a first-order Taylor approximation of the dynamic equations. The proposed frequency-domain model extends the quasi-static model to higher frequencies, while employing *dq*0 signals that are static at steady-state, and therefore combines the advantages of high bandwidth and a well-defined operating point. The standard quasi-static model follows as a special case from the model at low frequencies.

The paper continues as follows. Section 2 recalls basic concepts of dynamic phasors and explains how to formulate quasi-static models in terms of *dq*0 quantities. Section 3 presents the proposed *dq*0 model. The first-order *dq*0 model is presented in Section 4. Section 5 provides simple illustrative examples, followed by various numerical results provided in Section 6. Concluding remarks are drawn in Section 7.

2. Dynamic phasors in the *dq*0 reference frame

For systems in steady-state, the *dq*0 transformation maps sinusoidal signals to constant quantities. This transformation is compatible with standard electric machine models, and with emerging models of renewable and distributed generators [10,15,32,33].

Assume a general power network containing N three-phase units, with voltages and currents as presented in Fig. 1.

The *dq*0 transformation (as defined in [26]) is given by

$$\begin{bmatrix} x^d(t) \\ x^q(t) \\ x^0(t) \end{bmatrix} = \frac{2}{3} \begin{bmatrix} \cos(\omega_s t) & \cos\left(\omega_s t - \frac{2\pi}{3}\right) & \cos\left(\omega_s t + \frac{2\pi}{3}\right) \\ -\sin(\omega_s t) & -\sin\left(\omega_s t - \frac{2\pi}{3}\right) & -\sin\left(\omega_s t + \frac{2\pi}{3}\right) \\ \frac{1}{2} & \frac{1}{2} & \frac{1}{2} \end{bmatrix} \begin{bmatrix} x^a(t) \\ x^b(t) \\ x^c(t) \end{bmatrix}, \tag{1}$$

where ω_s is the nominal system frequency, and x is replaced with either a voltage (v_n) or a current (i_n) signal. A prominent feature of the *dq*0 transformation is that for *balanced* and *static* systems, the direct and quadrature components x^d, x^q are constants, and $x^0 = 0$. In a quasi-static system x^a, x^b, x^c are nearly sinusoidal, with slowly varying amplitudes and phases. In this case, the system can be modeled in terms of time-varying phasors, which are defined in terms of the *dq*0 components as

$$V_n(t) = \frac{1}{\sqrt{2}}\left(v_n^d(t) + jv_n^q(t)\right), \quad I_n(t) = \frac{1}{\sqrt{2}}\left(i_n^d(t) + ji_n^q(t)\right). \tag{2}$$

Under the quasi-static approximation these *dq* components are identical to the *xy* components, as described in [34]. The following analysis defines the standard quasi-static model and power flow equations in terms of *dq*0 signals. Quasi-static networks are usually described by the admittance matrix Y^{bus}. Define the vectors:

$$V^d(t) = \left[v_1^d(t), \ldots, v_N^d(t)\right]^{\mathrm{T}}, \quad I^d(t) = \left[i_1^d(t), \ldots, i_N^d(t)\right]^{\mathrm{T}}, \quad V^q(t) = \left[v_1^q(t), \ldots, v_N^q(t)\right]^{\mathrm{T}}, \quad I^q(t) = \left[i_1^q(t), \ldots, i_N^q(t)\right]^{\mathrm{T}},$$
$$V^0(t) = \left[v_1^0(t), \ldots, v_N^0(t)\right]^{\mathrm{T}}, \quad I^0(t) = \left[i_1^0(t), \ldots, i_N^0(t)\right]^{\mathrm{T}}. \tag{3}$$

Then the complex voltage and current phasors relate by

$$I^d(t) + jI^q(t) = Y^{bus}\left(V^d(t) + jV^q(t)\right) \tag{4}$$

and the real and imaginary parts of this equations are

$$I^d(t) = \mathrm{Re}\left\{Y^{bus}\right\} V^d(t) - \mathrm{Im}\left\{Y^{bus}\right\} V^q(t), \quad I^q(t) = \mathrm{Im}\left\{Y^{bus}\right\} V^d(t) + \mathrm{Re}\left\{Y^{bus}\right\} V^q(t). \tag{5}$$

These equations constitute a quasi-static model. Equivalently, quasi-static networks are also described by the power flow equations [33]

$$P_n(t) = |V_n(t)| \sum_{k=1}^{N} |y_{nk}||V_k(t)| \cos\left(\angle y_{nk} + \delta_k - \delta_n\right), \quad Q_n(t) = -|V_n(t)| \sum_{k=1}^{N} |y_{nk}||V_k(t)| \sin\left(\angle y_{nk} + \delta_k - \delta_n\right). \tag{6}$$

In which the constants y_{nk} are elements of the network admittance matrix Y^{bus}, and powers, amplitudes and phases are formulated in terms of $dq0$ signals as

$$P_n(t) = \mathrm{Re}\left\{V_n(t) I_n(t)^*\right\} = \frac{1}{2}\left(v_n^d(t) i_n^d(t) + v_n^q(t) i_n^q(t)\right), \quad Q_n(t) = \mathrm{Im}\left\{V_n(t) I_n(t)^*\right\} = \frac{1}{2}\left(v_n^q(t) i_n^d(t) - v_n^d(t) i_n^q(t)\right),$$
$$\left|V_n(t)\right| = \frac{1}{\sqrt{2}} \sqrt{\left(v_n^d(t)\right)^2 + \left(v_n^q(t)\right)^2}, \quad \delta_n(t) = \angle V_n(t) = \mathrm{atan2}\left(v_n^q(t), v_n^d(t)\right). \tag{7}$$

If the system is not quasi-static, the phasors above can be generalized by dynamic phasors. These can be defined by a Fourier series expansion, as in [16]. However, to simplify notations, we have chosen in this paper to define dynamic phasors with respect to the Fourier transform as

$$\begin{bmatrix} V_n^d(\omega) \\ V_n^q(\omega) \\ V_n^0(\omega) \end{bmatrix} = \int_{-\infty}^{\infty} \begin{bmatrix} v_n^d(t) \\ v_n^q(t) \\ v_n^0(t) \end{bmatrix} \mathrm{e}^{-j\omega t} \mathrm{d}t, \quad \begin{bmatrix} I_n^d(\omega) \\ I_n^q(\omega) \\ I_n^0(\omega) \end{bmatrix} = \int_{-\infty}^{\infty} \begin{bmatrix} i_n^d(t) \\ i_n^q(t) \\ i_n^0(t) \end{bmatrix} \mathrm{e}^{-j\omega t} \mathrm{d}t. \tag{8}$$

3. Large network dynamics in the *dq*0 reference frame

The power flow equations and the equivalent $dq0$ model in (5), (6) are only valid under the quasi-static approximation, assuming slow variations in amplitudes and phases [34]. The following theorem extends the quasi-static model to higher frequencies, and describes the system dynamics for general $dq0$ signals.

Theorem 1. *In symmetric power networks, a dynamic model based on dq0 dynamic phasors can be described as*

$$\begin{bmatrix} I^d(\omega) \\ I^q(\omega) \\ I^0(\omega) \end{bmatrix} = \begin{bmatrix} U(\omega) & jR(\omega) & 0 \\ -jR(\omega) & U(\omega) & 0 \\ 0 & 0 & Y^{bus}(\omega) \end{bmatrix} \begin{bmatrix} V^d(\omega) \\ V^q(\omega) \\ V^0(\omega) \end{bmatrix}. \tag{9}$$

The following definitions are used in (9):

$$U(\omega) := \frac{1}{2}\left(Y^{bus}(\omega + \omega_s) + Y^{bus}(\omega - \omega_s)\right), \quad R(\omega) := \frac{1}{2}\left(Y^{bus}(\omega + \omega_s) - Y^{bus}(\omega - \omega_s)\right), \tag{10}$$

and

$$V^d(\omega) = \left[V_1^d(\omega), \ldots, V_N^d(\omega)\right]^{\mathrm{T}}, I^d(\omega) = \left[I_1^d(\omega), \ldots, I_N^d(\omega)\right]^{\mathrm{T}}, \quad V^q(\omega) = \left[V_1^q(\omega), \ldots, V_N^q(\omega)\right]^{\mathrm{T}}, I^q(\omega) = \left[I_1^q(\omega), \ldots, I_N^q(\omega)\right]^{\mathrm{T}},$$
$$V^0(\omega) = \left[V_1^0(\omega), \ldots, V_N^0(\omega)\right]^{\mathrm{T}}, I^0(\omega) = \left[I_1^0(\omega), \ldots, I_N^0(\omega)\right]^{\mathrm{T}}. \tag{11}$$

Proof. Following the definition of the $dq0$ transformation in (1), voltages and currents can be expressed as sums of three elements

$$V^a(t) = V^d(t)\cos(\omega_s t) - V^q(t)\sin(\omega_s t) + V^0(t), \quad I^a(t) = I^d(t)\cos(\omega_s t) - I^q(t)\sin(\omega_s t) + I^0(t). \tag{12}$$

Similar expressions apply to phases b, c with a proper phase-shift of $\pm 2\pi/3$. Transformation to the frequency domain using the modulation property yields

$$V^a(\omega) = \frac{1}{2}\left(V^d(\omega - \omega_s) + V^d(\omega + \omega_s) + jV^q(\omega - \omega_s) - jV^q(\omega + \omega_s)\right) + V^0(\omega),$$
$$I^a(\omega) = \frac{1}{2}\left(I^d(\omega - \omega_s) + I^d(\omega + \omega_s) + jI^q(\omega - \omega_s) - jI^q(\omega + \omega_s)\right) + I^0(\omega). \tag{13}$$

According to definition

$$\begin{bmatrix} I_1^a(\omega) & \cdots & I_N^a(\omega) \end{bmatrix}^{\mathrm{T}} = Y^{bus}(\omega) \begin{bmatrix} V_1^a(\omega) & \cdots & V_N^a(\omega) \end{bmatrix}^{\mathrm{T}}. \tag{14}$$

Substituting (14) in (13) yields

$$I^d(\omega - \omega_s) + I^d(\omega + \omega_s) + jI^q(\omega - \omega_s) - jI^q(\omega + \omega_s) + 2I^0(\omega)$$
$$= Y^{bus}(\omega)\left(V^d(\omega - \omega_s) + V^d(\omega + \omega_s) + jV^q(\omega - \omega_s) - jV^q(\omega + \omega_s) + 2V^0(\omega)\right). \tag{15}$$

Using relation (10), equation (15) can be rewritten as

$$I^d(\omega-\omega_s)+I^d(\omega+\omega_s)+jI^q(\omega-\omega_s)-jI^q(\omega+\omega_s)+2I^0(\omega)=2Y^{bus}(\omega)V^0(\omega)+U(\omega-\omega_s)V^d(\omega-\omega_s)+jR(\omega-\omega_s)V^q(\omega-\omega_s)$$
$$+U(\omega+\omega_s)V^d(\omega+\omega_s)+jR(\omega+\omega_s)V^q(\omega+\omega_s)+j(-jR(\omega-\omega_s)V^d(\omega-\omega_s)+U(\omega-\omega_s)V^q(\omega-\omega_s))-j(-jR(\omega+\omega_s)V^d(\omega+\omega_s)$$
$$+U(\omega+\omega_s)V^q(\omega+\omega_s)), \tag{16}$$

which after comparison of coefficients results in (9). □

Note that Theorem 1 holds for symmetric networks, in which the matrix $Y^{bus}(\omega)$ equally applies to each of the three phases. However, the generators and loads connected to the network are not necessarily linear or symmetric.

The following corollary relates the proposed $dq0$ model to the standard quasi-static model.

Corollary 1. *When $Y^{bus}(\omega+\omega_s)=Y^{bus}$ and $Y^{bus}(\omega-\omega_s)=(Y^{bus})^*$, equation (9) reduces to the quasi-static expressions in (5).*

This corollary states that if the general $Y^{bus}(\omega+\omega_s)$ can be approximated by a constant matrix when $\omega\to 0$, then the dynamic model is quasi-static.

4. The first-order *dq*0 model

Since the full $dq0$ model in (9) is, in general, hard to implement numerically, this section presents a simplified version of it called the first-order $dq0$ model, which is obtained by a first-order Taylor approximation of the dynamic equations. In this case it is assumed that the $dq0$ signals are bandlimited, and have significant energy only at low frequencies. This enables representation of the admittance matrix by a Taylor series around $\omega=0$ as

$$\begin{aligned} Y^{bus}(\omega+\omega_s) &\approx \sum_{k=0}^{M}\frac{\omega^k}{k!}\frac{\partial Y^{bus}(\omega+\omega_s)}{\partial\omega^k}|_{\omega=0},\\ Y^{bus}(\omega-\omega_s) &\approx \sum_{k=0}^{M}\frac{\omega^k}{k!}\frac{\partial Y^{bus}(\omega-\omega_s)}{\partial\omega^k}|_{\omega=0}, = \sum_{k=0}^{M}(j\omega)^k\frac{j^k}{k!}\left(\frac{\partial Y^{bus}(\omega+\omega_s)}{\partial\omega^k}\right)^*|_{\omega=0},\\ Y^{bus}(\omega) &\approx \sum_{k=0}^{M}\frac{\omega^k}{k!}\frac{\partial Y^{bus}(\omega)}{\partial\omega^k}|_{\omega=0}, \end{aligned} \tag{17}$$

where in the expression for $Y^{bus}(\omega-\omega_s)$ we have utilized $Y^{bus}(\omega)=(Y^{bus}(-\omega))^*$ and employed nested functions derivatives. The standard quasi-static approximation is obtained by a zero-order Taylor series with $M=0$ such that

$$Y^{bus}(\omega+\omega_s)\approx Y^{bus}(\omega_s),\quad Y^{bus}(\omega-\omega_s)\approx\left(Y^{bus}(\omega_s)\right)^*. \tag{18}$$

If these expressions are substituted into the original model (9), then the model reduces to the quasi-static equations in (5). A more accurate dynamic model is obtained by the first-order Taylor series approximation ($M=1$) as

$$Y^{bus}(\omega+\omega_s)\approx Y^{bus}(\omega_s)+j\omega F,\quad Y^{bus}(\omega-\omega_s)\approx(Y^{bus}(\omega_s))^*+j\omega F^*,\quad Y^{bus}(\omega)\approx Y^{bus}(0)+j\omega F_0,\quad F=-j\frac{\partial Y^{bus}(\omega+\omega_s)}{\partial\omega}|_{\omega=0},$$
$$F_0=-j\frac{\partial Y^{bus}(\omega)}{\partial\omega}|_{\omega=0}. \tag{19}$$

Substitution of these expressions in (9) yields

$$\begin{bmatrix} I^d(\omega)\\ I^q(\omega)\\ I^0(\omega)\end{bmatrix}=(M_2+M_1j\omega)\begin{bmatrix} V^d(\omega)\\ V^q(\omega)\\ V^0(\omega)\end{bmatrix} \tag{20}$$

with

$$M_1=\begin{bmatrix}\mathrm{Re}\{F\} & -\mathrm{Im}\{F\} & 0\\ \mathrm{Im}\{F\} & \mathrm{Re}\{F\} & 0\\ 0 & 0 & F_0\end{bmatrix},\quad M_2=\begin{bmatrix}\mathrm{Re}\left\{Y^{bus}(\omega_s)\right\} & -\mathrm{Im}\left\{Y^{bus}(\omega_s)\right\} & 0\\ \mathrm{Im}\left\{Y^{bus}(\omega_s)\right\} & \mathrm{Re}\left\{Y^{bus}(\omega_s)\right\} & 0\\ 0 & 0 & Y^{bus}(0)\end{bmatrix}. \tag{21}$$

This model can be implemented in practice using a linear state-space model

$$\begin{aligned}\frac{dx}{dt} &= Ax+Bu\\ y &= Cx+Du,\end{aligned} \tag{22}$$

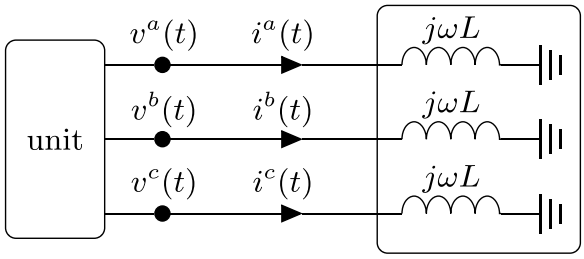

Fig. 2. Example 1: a network with a single inductor.

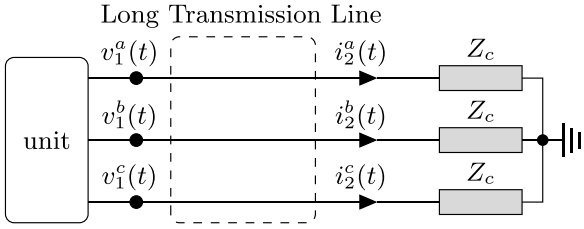

Fig. 3. Example 2: long transmission line feeding a matched load.

where $u=(V^d(t),V^q(t),V^0(t))^{\mathrm{T}}$, $y=(I^d(t),I^q(t),I^0(t))^{\mathrm{T}}$. The matrices A, B, C, D are chosen such that at low frequencies the frequency response of the state-space model (22) is equal to (20). The general frequency response is given by $y(\omega)=(C(j\omega I-A)^{-1}B+D)u(\omega)$, and is approximated at $\omega\to 0$ by

$$\begin{aligned} y(\omega) &\approx \left(C\left(-A^{-1}\left(I+j\omega A^{-1}\right)\right)B+D\right)u(\omega) \\ &= \left(-CA^{-1}B+D-j\omega CA^{-2}B\right)u(\omega). \end{aligned} \tag{23}$$

Comparison of (23) and (20) provides

$$-CA^{-2}B=M_1,\quad -CA^{-1}B+D=M_2. \tag{24}$$

From (24), C, D can be computed for any full-rank matrices A, B as

$$C=-M_1B^{-1}A^2,\quad D=M_2-M_1B^{-1}AB. \tag{25}$$

The matrices A, B can be arbitrarily chosen. It is typically beneficial to select A, B such that $D=0$, to obtain zero gain at $\omega\to\infty$. This criterion results in

$$D=M_2-M_1B^{-1}AB\Rightarrow A=BM_1^{-1}M_2B^{-1}. \tag{26}$$

In general, if the matrix M_1 is not full-rank, then A can be computed by solving a standard least-squares minimization problem

$$A=BPB^{-1},\quad P=\underset{X}{arg\,min}\|M_1X-M_2\|_2^2. \tag{27}$$

The matrix B can be arbitrarily chosen, for instance $B=I$.

5. Dynamic *dq*0 models: simple examples

The simple network in Fig. 2 demonstrates the difference between the quasi-static model and the full $dq0$ model.
In this example, the quasi-static model (5) provides

$$V^d(\omega)=-\omega_sLI^q(\omega),\quad V^q(\omega)=\omega_sLI^d(\omega). \tag{28}$$

In comparison, the $dq0$ model can be computed by (9), and results in

$$V^d(\omega)=j\omega LI^d(\omega)-\omega_sLI^q(\omega),\quad V^q(\omega)=\omega_sLI^d(\omega)+j\omega LI^q(\omega),\quad V^0(\omega)=j\omega LI^0(\omega). \tag{29}$$

Note that when $\omega\to 0$ the quasi-static and the $dq0$ models are equivalent.

Another example (Fig. 3) is the long transmission line. In this example the $dq0$ dynamic phasors are shown to relate through time delays. Assume a long power line of length l. The line is lossless, with inductance L_x and capacitance C_x per unit length. It feeds a matched load with an impedance equal to the characteristic impedance $Z_c=\sqrt{L_x/C_x}$. The resulting load current is delayed in respect to the source voltage [33] as

$$i_2^{abc}(t)=\frac{1}{Z_c}v_1^{abc}(t-d), \tag{30}$$

where the time delay is given by $d=l\sqrt{L_xC_x}$.

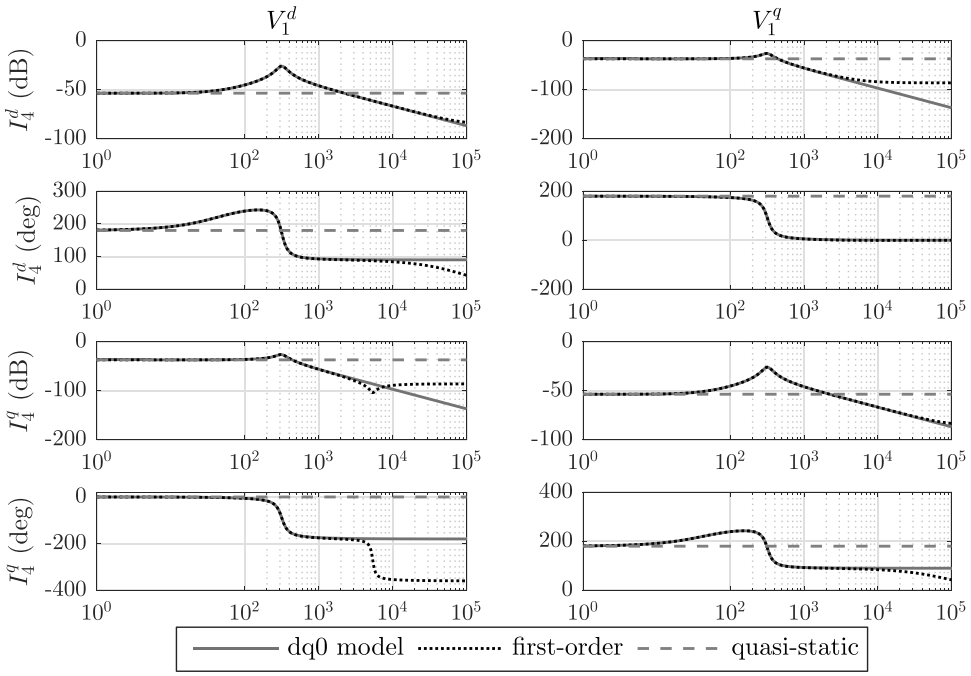

Fig. 4. Comparison of frequency responses in the 9-bus network for *dq* quantities from input 1 to output 4.

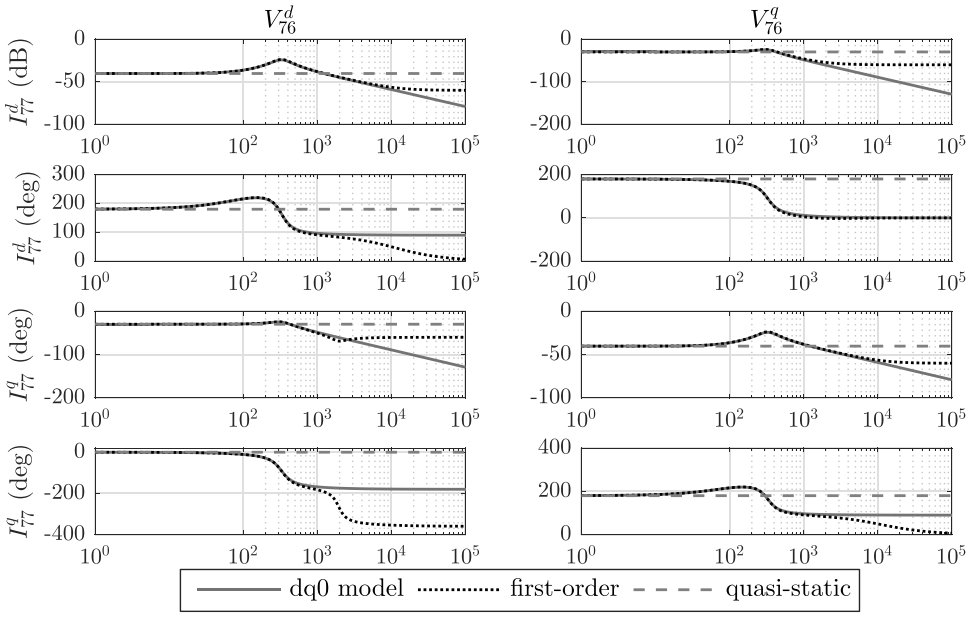

Fig. 5. Comparison of frequency responses in the 118-bus network for *dq* quantities from input 76 to output 77.

The corresponding *dq*0 model can be computed by (9). Defining $Y^{bus}(\omega)=(1/Z_c)e^{-j\omega d}$ and applying the inverse Fourier transform, the result is

$$i_2^d(t)=\frac{1}{Z_c}\left(\cos(\omega_s d)v_1^d(t-d)+\sin(\omega_s d)v_1^q(t-d)\right),\quad i_2^q(t)=\frac{1}{Z_c}\left(-\sin(\omega_s d)v_1^d(t-d)+\cos(\omega_s d)v_1^q(t-d)\right),\quad i_2^0(t)=\frac{1}{Z_c}v_1^0(t-d). \quad (31)$$

The direct and quadrature current components are delayed in respect to the source voltage.

6. Numerical results

In this section the various models are compared in terms of frequency and transient responses. Three models are tested: the full *dq*0 model, the first-order model, and the quasi-static model. These are compared to the full transient model, which is constructed in state-space using Matlab's Simscape Power Systems software package. The 9-, 30-, and 118-bus networks from the MatPower database [35] are used.

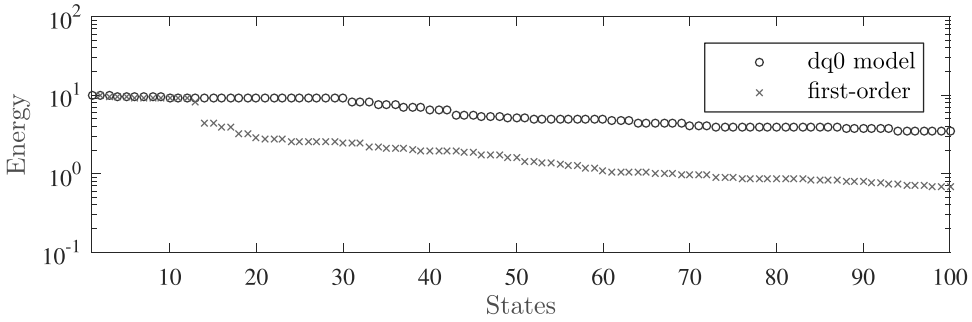

Fig. 6. Comparison of the first 100 largest Hankel singular values of the $dq0$ model and the first-order model in the 118-bus network.

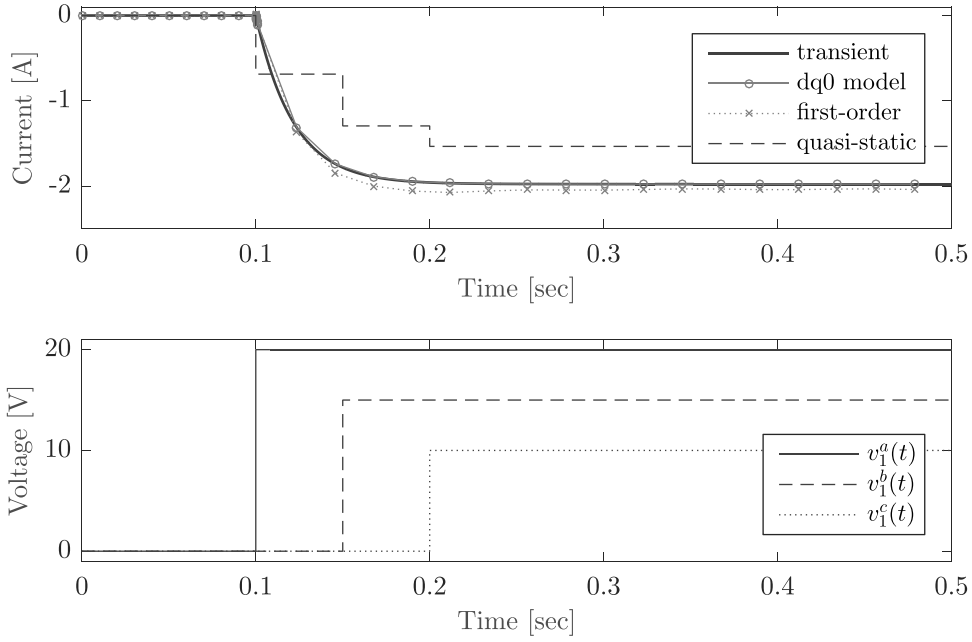

Fig. 7. Comparison of step-responses in the 9-bus system. The inputs (bottom plot) are steps in phases a, b, c at bus 1. The output is the current of phase a at bus 4.

An array of Bode plots representing the $dq0$, first-order, and quasi-static models is graphically illustrated in Figs. 4 and 5 for 9- and 118-bus networks. The plots depict the magnitude (in dB) and phase (in degrees) for several input/output pairs. The step input is applied to a generator located at bus 1 and the output is measured at bus 4 for the case of 9-bus network. Similarly, for 118-bus network the step input is applied to a generator located at bus 76 and the output is measured at bus 77. The figures show that the frequency responses coincide at low frequencies ($\omega \to 0$) and diverge at high frequencies. Specifically, the quasi-static model is represented by a constant gain, and has a constant gain and phase at all frequencies. The first-order model response coincides with the $dq0$ model response over a wider frequency range and deviates only at high frequencies. These figures illustrate the main result presented in Theorem 1 that $dq0$ model extends both quasi-static and first-order models by taking high-frequency dynamic phenomena into account.

Fig. 6 compares the largest singular values of the $dq0$ model and the first-order model for the 118-bus network. It can be seen that the most energetic (largest) values are similar, meaning that the majority of energy is preserved. This in turn verifies the quality of the first-order model.

Figs. 7–11 compare the transient response of the various models for the 9-, 30- and 118-bus networks. All inputs and outputs are three phase signals. The transient model is simulated directly in the abc reference frame. The $dq0$ model, quasi-static model, and the first-order model are represented in the $dq0$ reference frame, so input and output signals are converted accordingly using (1). To this end, the $dq0$ model is represented in the state-space form using implementation available in [36]. The first-order model is implemented using equations (22)–(27).

Figs. 7 and 8 provide simulation results for the case of 9-bus network. In Fig. 7 the step input signals (shifted in time for each of the phases) are applied to the generator 1 at bus 1 and the outputs are measured at bus 4. In Fig. 8 a more complicated scenario is considered. Before the transient, the inputs are balanced three phase sinusoidal signals $u_1^a = \sin(2\pi 50t)$ at bus 1. Then, the transient is triggered by shorting phase a to ground, i.e., $u_1^a = 0$. Note that $u_1^{c,d} = \sin(2\pi 50t \pm 2\pi/3)$. The output is the current of phase a measured at bus 4. The simulation results confirm the above frequency domain analysis presented in Fig. 4 and the fact that the quasi-static model becomes inaccurate at high frequencies. The similar settings were used to obtain simulation results for the 30- and 118-bus networks (see Figs. 9–11). The figures show that transient responses of the $dq0$ models are similar to those of the transient models. The quasi-static model is implemented by constant gains, and is inaccurate, except for balanced sinusoidal inputs. The first-order model is moderately accurate.

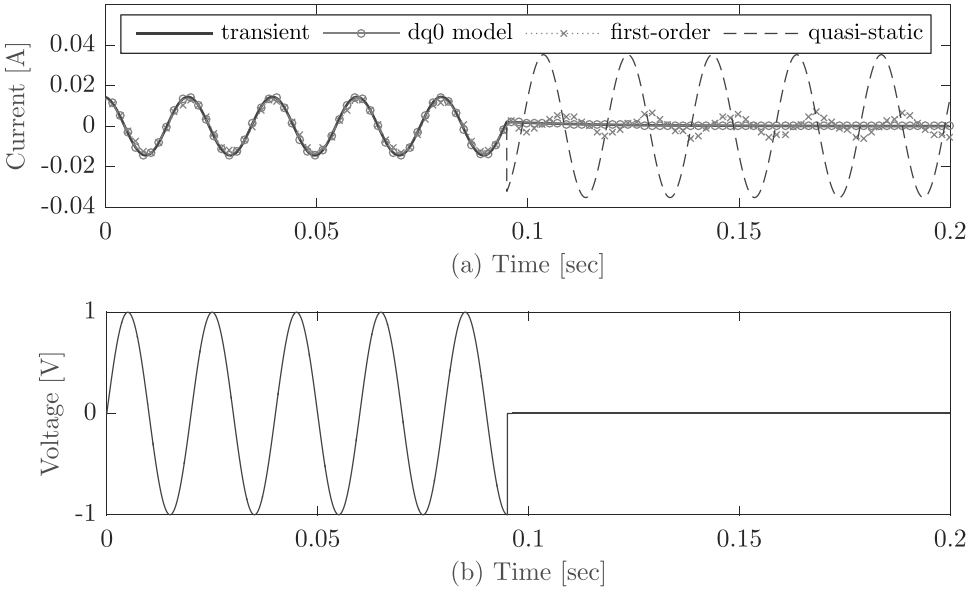

Fig. 8. Comparison of transients in the 9-bus system. Before the transient, the inputs are balanced three phase sinusoidal signals at bus 1. The transient is triggered by shorting phase *a* to ground. The output is the current of phase *a* at bus 4.

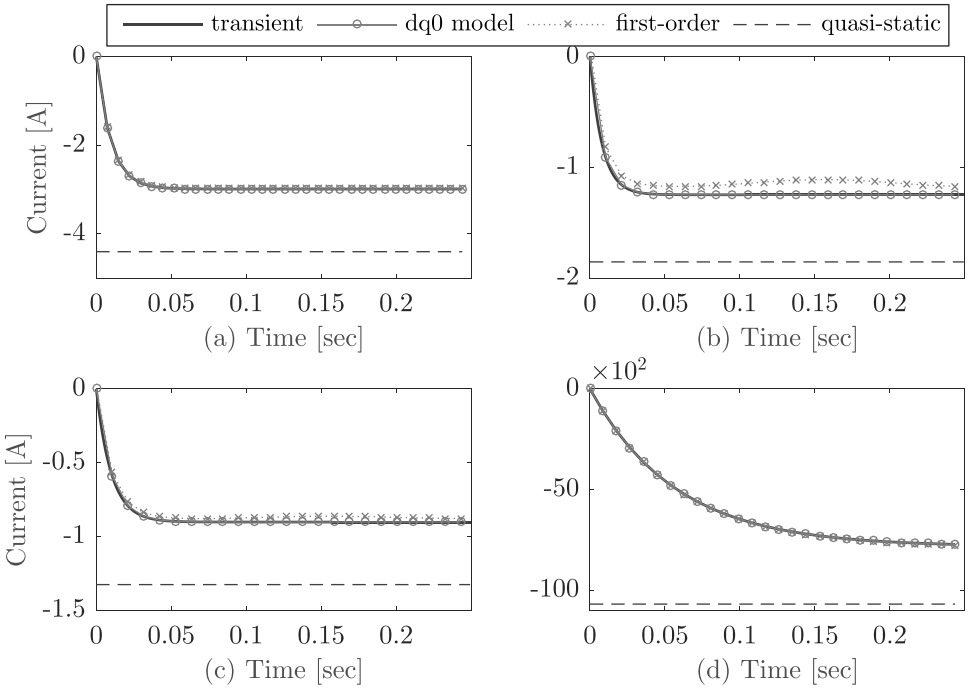

Fig. 9. Comparison of step responses in the 30-bus network. The inputs are steps at $t = 0$ in phases *a*, *b*, *c*. (a) input at bus 1, output at bus 2, (b) input at bus 5, output at bus 7, (c) input at bus 8, output at bus 28, (d) input at bus 11, output at bus 9.

Table 1
Errors in transient responses.

		Fig. 7	Fig. 8(a)	Fig. 10	Fig. 11(a)
MSE	*dq*0	0.9595×10^{-8}	0.9572×10^{-9}	0.6557×10^{-8}	0.9340×10^{-7}
	fo	0.0035	3.4425×10^{-5}	4.6116×10^{-5}	4.9407×10^{-4}
	qs	0.1929	0.0020	0.0039	0.0170
ISE	*dq*0	0.7922×10^{-8}	0.9706×10^{-9}	0.3570×10^{-8}	0.8491×10^{-7}
	fo	0.0035	3.4446×10^{-5}	1.1498×10^{-5}	1.2363×10^{-4}
	qs	0.1913	0.0020	9.6554×10^{-4}	0.0042

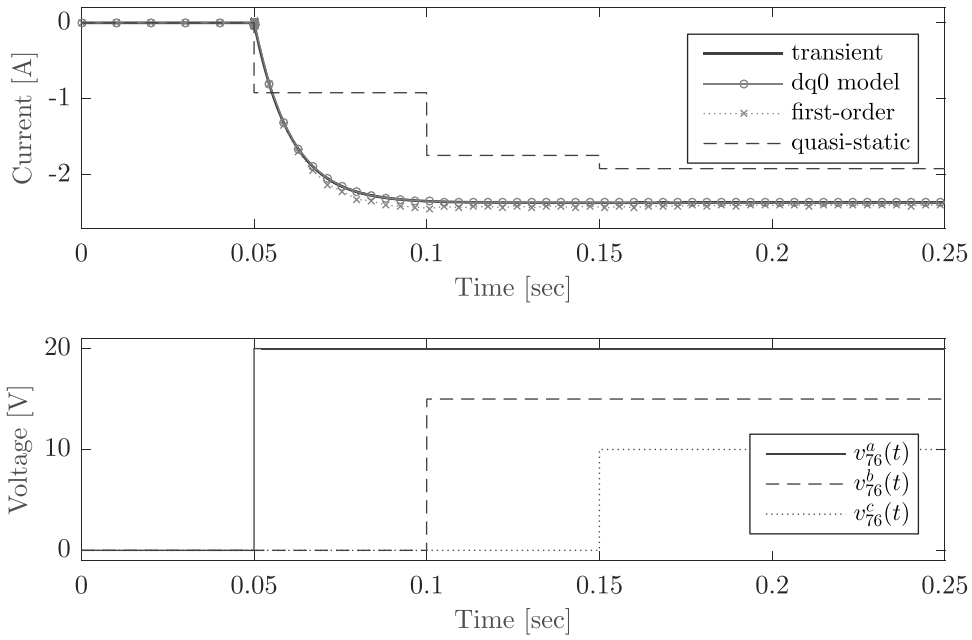

Fig. 10. Comparison of step-responses in the 118-bus system. The inputs (bottom plot) are steps in phases *a*, *b*, *c* of bus 76. The output is the current of phase *a* at bus 77.

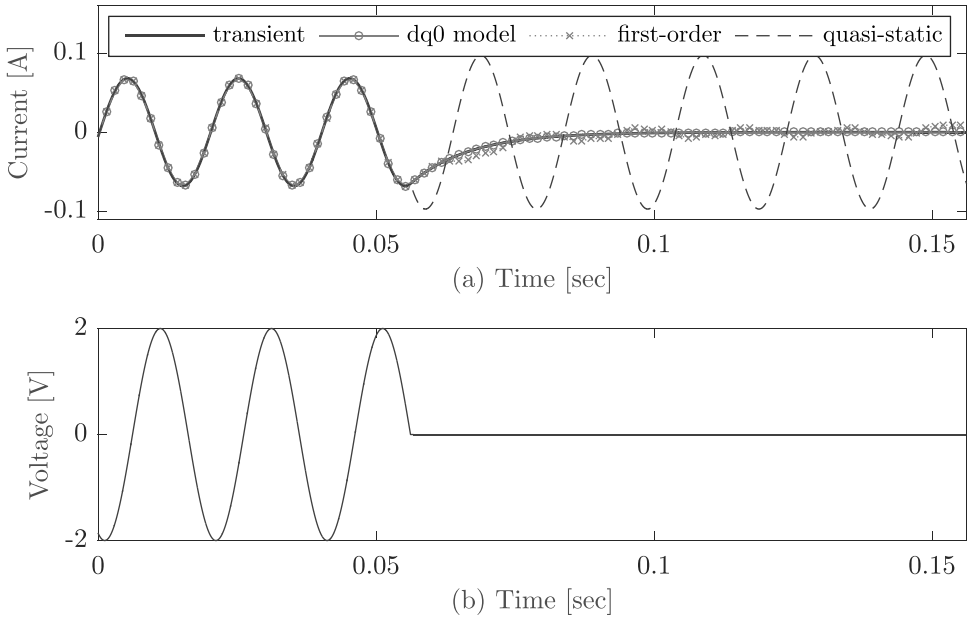

Fig. 11. Comparison of transients in the 118-bus system. Before the transient, the inputs are balanced three phase sinusoidal signals at bus 76. The transient is triggered by shorting phase *a* to ground. The output is the current of phase *a* at bus 77.

Errors in the models transient responses are presented in Table 1, where two typical metrics, the mean squared error (MSE) and the integral squared error (ISE), are used. The errors are calculated in comparison to the transient model, which serves as a reference. It can be seen that the magnitudes of errors for the *dq*0 model are significantly lower than those of first-order and quasi-static models.

7. Conclusion

Dynamic behavior and stability of large-scale power systems have been traditionally studied by means of time-varying phasors, under the assumption that the system is quasi-static. However, with increasing integration of fast renewable and distributed sources into power grids, this assumption is becoming increasingly inaccurate. This paper uses dynamic phasors in the *dq*0 reference frame to describe the dynamics of large transmission and distribution networks. The proposed models do not employ the assumption of quasi-static phasors, and therefore remain accurate over a wide range of frequencies. The full *dq*0 model is based on the frequency dependent admittance matrix, and is approximated using the Taylor series expansion to generate models of lower complexity: the classic quasi-static model is obtained by a zero-order approximation, while the more accurate first-order model is obtained by a first-order approximation. The developed models combine two properties of interest. On one hand, they provide the advantages of the *dq*0 reference frame. Specifically,

the models employ nonrotating *dq*0 signals that are static at steady-state, and thus enable a well-defined operating point. On the other hand, the proposed models improve the accuracy of the quasi-static model at high frequencies, enabling representation of fast dynamic phenomena in networks that include small distributed generators and fast power electronics based devices. In particular, these properties can contribute to accurate and low complexity stability analysis in such networks. Simulations show that the frequency responses of all models coincide at low frequencies and diverge at high frequencies. In addition, responses of the *dq*0 model in the time domain and in the *abc* reference frame are very close to those of the transient model.

Acknowledgment

The work was partly supported by Grand Technion Energy Program (GTEP) and a Technion fellowship.

References

[1] Y. Liu, K. Sun, Y. Liu, A measurement-based power system model for dynamic response estimation and instability warning, Electr. Power Syst. Res. 124 (2015) 1–9.
[2] L. Miller, L. Cibulka, M. Brown, A.V. Meier, Electric distribution system models for renewable integration: Status and research gaps analysis, Tech. rep., California Energy Commission, CA, USA, 2013.
[3] P.M. Anderson, A.A. Fouad, Power System Control and Stability, John Wiley & Sons, 2008.
[4] C. Dufour, J. Mahseredjian, J. Bélanger, A combined state-space nodal method for the simulation of power system transients, IEEE Trans. Power Del. 26 (2) (2011) 928–935.
[5] U.N. Gnanarathna, A.M. Gole, R.P. Jayasinghe, Efficient modeling of modular multilevel HVDC converters (MMC) on electromagnetic transient simulation programs, IEEE Trans. Power Del. 26 (1) (2011) 316–324.
[6] R. Majumder, Some aspects of stability in microgrids, IEEE Trans. Power Syst. 28 (3) (2013) 3243–3252.
[7] T. Nishikawa, A.E. Motter, Comparative analysis of existing models for power-grid synchronization, New J. Phys. 17 (1) (2015).
[8] R. Zárate-Mi nano, T.V. Cutsem, F. Milano, J.A. Conejo, Securing transient stability using time-domain simulations within an optimal power flow, IEEE Trans. Power Syst. 25 (1) (2010) 243–253.
[9] M. Ilić, J. Zaborszky, Quasistationary phasor concepts, in: Dynamics and Control of Large Electric Power Systems, Wiley, New York, 2000, pp. 9–60.
[10] P.C. Stefanov, A.M. Stanković, Modeling of UPFC operation under unbalanced conditions with dynamic phasors, IEEE Trans. Power Syst. 17 (2) (2002) 395–403.
[11] R. Yousefian, S. Kamalasadan, A Lyapunov function based optimal hybrid power system controller for improved transient stability, Electr. Power Syst. Res. 137 (2016) 6–15.
[12] A.M. Stanković, S.R. Sanders, T. Aydin, Dynamic phasors in modeling and analysis of unbalanced polyphase A machines, IEEE Trans. Energy Convers. 17 (1) (2002) 107–113.
[13] S. Almer, U. Jonsson, Dynamic phasor analysis of periodic systems, IEEE Trans. Autom. Control 54 (8) (2009) 2007–2012.
[14] M. Daryabak, S. Filizadeh, J. Jatskevich, A. Davoudi, M. Saeedifard, V.K. Sood, J.A. Martinez, D. Aliprantis, J. Cano, A. Mehrizi-Sani, Modeling of LCC-HVDC systems using dynamic phasors, IEEE Trans. Power Del. 29 (4) (2014) 1989–1998.
[15] T. Demiray, G. Andersson, L. Busarello, Evaluation study for the simulation of power system transients using dynamic phasor models, in: Transmission and Distribution Conf. and Expo, Bogotá, Colombia, 2008, pp. 1–6.
[16] A.M. Stanković, T. Aydin, Analysis of asymmetrical faults in power systems using dynamic phasors, IEEE Trans. Power Syst. 15 (3) (2000) 1062–1068.
[17] C. Liu, A. Bose, P. Tian, Modeling and analysis of HVDC converter by three-phase dynamic phasor, IEEE Trans. Power Del. 29 (1) (2014) 3–12.
[18] H. Zhu, Z. Cai, H. Liu, Q. Qi, Y. Ni, Hybrid-model transient stability simulation using dynamic phasors based HVDC system model, Electr. Power Syst. Res. 76 (6-7) (2006) 582–591.
[19] M.C. Chudasama, A.M. Kulkarni, Dynamic phasor analysis of SSR mitigation schemes based on passive phase imbalance, IEEE Trans. Power Syst. 26 (3) (2011) 1668–1676.
[20] P. Mattavelli, A.M. Stankovic, G.C. Verghese, SSR analysis with dynamic phasor model of thyristor-controlled series capacitor, IEEE Trans. Power Syst. 14 (1) (1999) 200–208.
[21] Z. Miao, L. Piyasinghe, J. Khazaei, L. Fan, Dynamic phasor-based modeling of unbalanced radial distribution systems, IEEE Trans. Power Syst. 30 (6) (2015) 3102–3109.
[22] S. Chandrasekar, R. Gokaraju, Dynamic phasor modeling of type 3 DFIG wind generators (including SSCI phenomenon) for short-circuit calculations, IEEE Trans. Power Del. 30 (2) (2015) 887–897.
[23] T.H. Demiray, Simulation of power system dynamics using dynamic phasor models. Ph.D. thesis, TU Wien, 2008.
[24] T. Yang, S. Bozhko, G. Asher, Multi-generator system modelling based on dynamic phasor concept, in: European Conf. on Power Electronics and Applications, Lille, France, 2013, pp. 1–10.
[25] T. Bi, H. Liu, Q. Feng, C. Qian, Y. Liu, Dynamic phasor model-based synchrophasor estimation algorithm for M-class PMU, IEEE Trans. Power Del. 30 (3) (2015) 1162–1171.
[26] D.-G. Lee, S.-H. Kang, S.-R. Nam, Modified dynamic phasor estimation algorithm for the transient signals of distributed generators, IEEE Trans. Smart Grids 4 (1) (2013) 419–424.
[27] R.K. Mai, L. Fu, Z.Y. Dong, K.P. Wong, Z.Q. Bo, H.B. Xu, Dynamic phasor and frequency estimators considering decaying DC components, IEEE Trans. Power Syst. 27 (2) (2012) 671–681.
[28] R.K. Mai, L. Fu, Z.Y. Dong, B. Kirby, Z.Q. Bo, An adaptive dynamic phasor estimator considering DC offset for PMU applications, IEEE Trans. Power Del. 26 (3) (2011) 1744–1754.
[29] J. Ren, M. Kezunovic, An adaptive phasor estimator for power system waveforms containing transients, IEEE Trans. Power Del. 27 (2) (2012) 735–745.
[30] T. Yang, S. Bozhko, J.M. Le-Peuvedic, G. Asher, C.I. Hill, Dynamic phasor modeling of multi-generator variable frequency electrical power systems, IEEE Trans. Power Syst. 31 (1) (2016) 563–571.
[31] X. Guo, Z. Lu, B. Wang, X. Sun, L. Wang, J.M. Guerrero, Dynamic phasors-based modeling and stability analysis of droop-controlled inverters for microgrid applications, IEEE Trans. Smart Grids 5 (6) (2014) 2980–2987.
[32] A.E. Fitzgerald, C. Kingsley, S.D. Umans, Electric Machinery, 6th ed., McGraw-Hill, New York, 2003.
[33] J.J. Grainger, W.D. Stevenson, Power System Analysis, McGraw-Hill, New York, 1994.
[34] T.V. Cutsem, C. Vournas, Voltage Stability of Electric Power Systems, Kluwer Academic Publishers, Norwell, MA, 1998.
[35] R.D. Zimmerman, C.E. Murillo-Sánchez, R.J. Thomas, MATPOWER: steady-state operations planning and analysis tools for power systems research and education, IEEE Trans. Power Syst. 26 (1) (2011) 12–19.
[36] Y. Levron, J. Belikov, Toolbox for modeling and analysis of power networks in the *dq*0 reference frame, MATLAB Central File Exchange, 2016 http://www.mathworks.com/matlabcentral/fileexchange/58702 (retrieved 15.08.16).